# Stochastic Simulation of Benign Avascular Tumour growth using the Potts Model.

Emma L. Stott[1], Nick F. Britton
Department of Mathematical Sciences, University of Bath, Claverton Down, Bath. BA2 7AY. England.

James A. Glazier, Mark Zajac
Department of Physics, University of Notre Dame, Notre Dame, IN 46556. U.S.A.

## Abstract

We simulate the growth of a benign avascular tumour embedded in normal tissue, including cell sorting that occurs between tumour and normal cells, due to the variation of adhesion between different cell types.

The simulation uses the Potts Model, an energy minimisation method. Trial random movements of cell walls are checked to see if they reduce the adhesion energy of the tissue. These trials are then accepted with Boltzmann weighted probability.

The simulated tumour initially grows exponentially, then forms three concentric shells as the nutrient level supplied to the core by diffusion decreases: the outer shell consists of live proliferating cells, the middle of quiescent cells and the centre is a necrotic core, where the nutrient concentration is below the critical level that sustains life. The growth rate of the tumour decreases at the onset of shell formation in agreement with experimental observation. The tumour eventually approaches a steady state, where the increase in volume due to the growth of the proliferating cells equals the loss of volume due to the disintegration of cells in the necrotic core. The final thickness of the shells also agrees with experiment.

**Keywords:** Simulation of avascular tumour growth - Potts model - Differential adhesion - Proliferation.

[1]To whom correspondence should be directed. e-mail: els@maths.bath.ac.uk

# 1 Introduction

## 1.1 Tumour Growth

A tumour is an abnormal mass of tissue, whose growth rate exceeds and is uncoordinated with that of surrounding normal tissues [1].

Tumours usually start as a mild disorder of cell behaviour that may develop slowly into a full blown cancer. The progression from the earliest induction event to the clinically recognisable tumour can take many years and the formation of a tumour is the exception, not the rule for transformed cells. Part of the reason for this long period is that the cells have to undergo a number of changes before they become hyperplastic and then truly cancerous [2]. Cancer cells require a particular developmental pathway. One of these requirements is to become immortal and acquire the ability to undergo almost unlimited divisions [3]. To do so the cell must ignore extracellular signals to halt cell division (both chemical and contact) and must also avoid the natural limit to the number of cell divisions caused by the exhaustion of telomeres [4, 5]. Normal cells have a very limited capacity for replication. For example, normal cells on a petri dish form a monolayer, growing until they reach the edges confluently, and then stop, whereas cancer cells carry on proliferating, lying across each other in a haphazard arrangement, no longer in a monolayer [1].

Apoptosis is an evolutionarily conserved, innate process by which cells destroy themselves by systematically inactivating, disassembling, and degrading their own structural and functional components [6]. In normal tissue, apoptosis deletes unnecessary, damaged and potentially harmful cells to ensure structural and functional homeostasis. Apoptosis occurs in nearly every cell type throughout development and maturation. Cancer cells appear to have defects in the regulation of genes (*e.g.* P53) that control apoptosis. These defects render the tumour cells resistant to the induction of apoptosis by a wide variety of stimuli, including chemotherapeutic drugs and radiotherapy [6] and also add to the cells' apparent immortality.

Tumours can be divided into two classes, benign or malignant, depending on their method of growth. Benign tumours grow by expansion, compressing or displacing surrounding normal tissue, while malignant tumours grow by local infiltration, destroying the tissue which they invade. Benign tumours grow at their site of origin only, but malignant tumours may spread to distant sites, with cells detaching from the primary tumour and migrating to remote sites via the blood stream, in the lymph nodes or across connective tissue. This process is known as metastasis and the secondary tumours formed are metastases. The majority of deaths from cancer are due to the formation of metastases at sites remote from the primary tumour.

Benign tumours may cause disease by compression of adjacent structures, or in certain circumstances by secretion of hormones. In contrast, malignant tumours always have the potential to cause death as a result of their aggressive growth and invasiveness.

The growth of solid tumours in animals always involves some vascularization, but the direct diffusion of nutrients and waste from and to surrounding tissue regulates the earliest stages of tumour development [7]. Experiments on the growth of nodular carcinomas *in vitro* [8, 9, 10], or isolated tumours *in vivo* [11, 12], show that the growth of a solid malignancy by diffusion alone leads asymptotically to a dormant but viable steady state. In this dormant state, the volume increase due to cell proliferation balances cell death and volume loss in the necrotic core. In our simplified model, we assume that the availability of a single, slow-diffusing nutrient is the primary limit on tumour growth, and that other nutrients and the diffusion of waste are sufficiently rapid that they do not limit the growth rate.

When the tumour is tiny, every cell receives sufficient nutrient by diffusion and the growth rate of the population is exponential [13]. The consumption of nutrient by the cells means that the concentration of nutrient decreases towards the centre of the tumour, as it is only supplied to the periphery.

As the tumour grows, supplying the nutrient to the central core by diffusion becomes more and more difficult, so that the core nutrient concentration diminishes. Eventually, the concentration falls below the critical level at which cells become quiescent; alive, but no longer proliferating. If the nutrient level near these cells increases above the critical level, they reenter the proliferation cycle [14]. Many studies show that microenvironmental factors, such as $O_2$ and nutrient supply, as well as accumulation of metabolic wastes, greatly influence cell metabolism [15]. When quiescent cells appear, the growth of the tumour slows down to become linear [16, 17], because part of the tumour volume is no longer involved in the production of new cells.

The tumour then grows until it reaches another critical size, where the nutrient concentration at the centre is not high enough to sustain life. At this stage, a necrotic core forms. This core contains cells in varying stages of disintegration. Dead cells break down into chemical compounds which are freely permeable through cell membranes. The mass or cell volume lost this way is replaced by cells pushed inward by the forces of adhesion and surface tension in the tumour. Some cells, newly generated on the surface of the tumour, gradually migrate toward the core [18]. Cells can also migrate outward by diffusion due to membrane fluctuations. The growth rate decreases rapidly when the necrotic core forms because it becomes increasingly difficult to obtain nourishment and dispose of waste solely by diffusion. As the tumour continues to grow and develop, the outer shell of dividing cells becomes roughly constant in size - about 1-3 cells thick .

Eventually, the necrotic disintegration, accumulation of mitotic wastes [19] and mitotic inhibitory factors [20] reduce the rate of growth so much that the overall volume of the tumour remains constant [9, 13, 21]. Although the tumour volume is in equilibrium, the cells in the outer shell still proliferate. But, the volume lost through necrotic disintegration cancels the volume produced by mitosis.

The typical steady state configuration of an avascular tumour is a sphere, a few millimetres in diameter, which histological examination shows to consist of three distinct concentric annular shells [13, 22, 23]. In the thin, outermost shell, the cells grow and divide as they do in the exponential phase. In the adjoining shell, typically three times as thick as the proliferating layer, the quiescent cells exhibit little or no proliferation. The innermost core consists of necrotic debris [18]. The tumour may remain in this dormant state for months or even years [24].

## 1.2 Cell Sorting

In a number of cell sorting experiments [25] -, cells migrate over distances much greater than one cell diameter in order to restore disrupted patterns or form new ones. The natural configuration of mesoderm, endoderm and ectoderm from amphibian embryos can be recovered from excised tissues combined in the right proportions [35]. When mixed together in suspension, chicken embryo neural and pigmented retinal cells precipitate to produce a disordered aggregate. The initially irregular aggregate rounds over time. Pigmented cells coalesce at the centre to form a sphere while neural cells organise to form an encompassing outer layer. Significantly, the outcome of sorting experiments is largely independent of the initial conditions [36]. An aggregate of neural cells rounds in isolation but spreads to engulf a pigmented cell aggregate if the two are placed in contact. Similarly, an intact fragment of chicken heart ventricle will envelope a chicken cartilage fragment. The coelenterate animal *Hydra vulgaris* [37, 38, 39] is basically a hollow cylinder with an extracellular matrix sandwiched between layers of endodermal and ectodermal cells. When dismantled at the cellular level, *hydra* can recover their original state and when turned in-side-out they are able to re-invert themselves. Mombach *et al.* [40, 41] showed that there was no long range interaction in their chick embryo experiments. These and other observations, suggest that an underlying mechanism for local cell sorting based on intrinsic cell properties rather than chemical gradients or the starting locations of cells in a tissue.

## 1.3 Differential Adhesion

Steinberg proposed the Differential Adhesion Hypothesis [25, 26, 27, 42] to explain cell sorting as a minimisation of contact energy at cell interfaces. Experiments [35, 43, 44] show that the strength of attachment between two cells which come into contact depends on the type of cells involved. The difference in adhesion energy results from the number and particular type of surface adhesion molecules present on the cell membrane. Classes of adhesion molecules include cadherins, N-CAM and many other varieties, some non-specifically adhesive, others, like N-CAM, extremely variable in sequence (and hence relative adhesivity) between cell types. Movement of a cell requires work against the adhesive forces of its neighbours under the constraint on cell volume imposed by membrane elasticity. Thus, affinity between neighbouring cells determines the energy of a cell aggregate. Interfaces between cells which have the potential to form stronger attachments with more amenable coupling partners store more energy. Cytoskeletal membrane fluctuations allow the cells in an aggregate to explore an abstract energy landscape randomly yet exhaustively. The local energy gradient directs cell movement, leading to a configuration with minimum energy. As jostling causes adhesion molecules to unbind and re-bind, strong bonds tend to replace weak bonds, making best use of the available binding surface and thereby maximising the work required to remove a cell from an aggregate. Differential adhesion plays an important role in cell recognition [29], gastrulation [45, 46], cell shaping [47], control of pattern formation [48] as well as cancer metastasis [49].

# 2 Computer Simulations

## 2.1 Overview and History

A cellular automaton simulation represents cells as one or more discrete units with rules to describe their interactions, emphasising supercellular processes. Continuum models are an alternative to solving the many body problem represented by cellular patterns. Emphasising spatial and temporal variation of fields, these methods describe cellular patterns in terms of density functions which satisfy second order nonlinear differential equations for diffusion and wave propagation. They stress the interaction of each cell with the global environment, but cannot easily identify individual cells.

Models in which the degrees of freedom reside on a lattice and interact locally arise in several areas of condensed matter physics and field theory. The simplest of these is the Ising model, which can be taken as a crude description of a magnetic material [50]. The Ising model is a two spin version of the *Potts Model*.

For example, using the magnetic language, the Ising model consists of a set of spin degrees of freedom interacting with each other and with an external magnetic field. In a biological cell simulation, using Ising or Potts models, the spins correspond to individual cells, with the spin number being the unique index number of the cell.

The large-Q Potts model (Q is the unique number of spins and cells) can be extended to combine discrete and continuum methods, describing multiple interactions between cells at multiple length scales. The Potts model was originally developed to simulate surface energy driven diffusion in non-biological patterns like the increase in mean grain size during annealing of polycrystalline aggregates [51, 52]. It accurately simulates the time evolution of experiments in metals and liquid foams [53, 54]. It can also simulate biological phenomena like the development of the slime mold, *Dictyostelium discoideum* [55], and growth of tissue [56, 57, 58].

The basic Potts model simulates a pure material with a single surface energy. Mismatched bonds between different cells (spins) have energy 1 and bonds between like spins have energy 0. The Hamiltonian is:

$$\mathcal{H}_{\text{Potts}} = \sum_{\substack{\text{neighbours} \\ (i,j)\ (i',j')}} (1 - \delta_{\sigma_{(i,j)}\sigma_{(i',j')}}),$$

where the neighbours, $(i, j)$ and $(i', j')$, may be of any desired range on either a square or hexagonal lattice. $\delta_{\sigma\sigma'}$ is the Krönicker $\delta$. At each step, a site is selected at random and its spin is changed from $\sigma$ to $\sigma'$ with Boltzmann probability, for a temperature $T > 0$,

$$P(\sigma(i,j) \rightarrow \sigma(i',j')) = \begin{cases} \exp(-\triangle\mathcal{H}/T) & \text{if } \triangle\mathcal{H} > 0 \\ 1 & \text{if } \triangle\mathcal{H} \leq 0, \end{cases}$$

where $\triangle\mathcal{H}$ is the energy gain/loss produced by the change. These dynamics allow cells to move slowly, by gradual adjustment of their boundary position. One Monte Carlo Step (MCS) is defined to be as many trials as the number of lattice sites.

## 2.2 The Extended Potts Model

The Extended Potts Model [59, 60, 61] uses a three-dimensional lattice with as many as $200^3$ elements partitioned into cells. Clustered array elements sharing a common value delineate regions belonging to different unique cells. A second label, shared by all domains of the same type, distinguishes cells from different tissues. Cells have a type dependent volume constraint which models membrane elasticity so that no single cell can grow or shrink without bound. The array can include a border of neighbouring sites assigned to a domain of unlimited volume. This large domain represents a medium in which the cells exist. A homogeneous slab of sites inserted at the base of the array can represent a substrate. With domains sufficiently large, cells and tissues are free to deform almost arbitrarily as the array evolves.

The patterns formed by cells and tissues correspond to an abstract stored energy. Contributions to the energy include a sum over the coupling between neighbouring array elements together with a sum over contributions from the membrane elasticity of each cell:

$$\begin{aligned}\mathcal{H} &= \sum_{\substack{\text{neighbours}\\(i,j,k)\ (i',j',k')}} J[\tau(\sigma_{(i,j,k)}),\tau(\sigma_{(i',j',k')})](1-\delta_{\sigma_{(i,j,k)}\sigma_{(i',j',k')}}) \\ &\qquad + \sum_{\substack{\text{all domains}\\ \lambda[\tau(\sigma)]\neq 0}} \lambda[\tau(\sigma)](v(\sigma)-V)^2\ ,\end{aligned}$$

where $\mathcal{H}$ is the total energy (the Hamiltonian), while domain $\sigma$ of type $\tau$ includes $\sigma_{(i,j,k)}$ as a constituent array element. Coupling strengths are defined for every possible pair of domain types. The coupling matrix elements $J[\tau,\tau']$ give the energy stored in a bond between a site and a neighbour. The sum over the whole lattice excludes neighbours within the same domain so that stored energy is localised at boundaries. For each cell, the volume under stress $v(\sigma)$ may differ from the target volume $V$ for undeformed cells. The sum over domains excludes domains of unconstrained volume for which the elasticity $\lambda_\tau$ is zero. Cell elasticity imposes a global constraint on cell volume while cell couplings determine the work required to cause local membrane deformations.

The organisation of cells and tissues develops in a probabilistic manner under Monte Carlo dynamics. An array element is chosen at random and provisionally reassigned to a neighbouring domain. A change in energy results since a modified site couples differently with its neighbours and volume transfers between domains. The chance of accepting reassignments is the same Boltzmann factor as in the standard Potts Model. The parameter $T$ controls the amplitude of cell membrane fluctuations. The possibility of accepting small energy gains allows cells to escape from locally stable configurations to find the configuration of absolute minimum energy. Experiments and simulations [62, 63] have shown that epithelial cells in tissues exhibit approximately Brownian motion and a roughly Maxwellian distribution of velocities consistent with statistical mechanical dynamics. Under repeated application of this algorithm, membrane curvature evolves realistically in response to gradual diffusion of domain boundaries within the array.

This model, with area constraints and differential adhesivity, can simulate experimental biological cell sorting quantitatively. Sorting shows a crossover between a rapid boundary-driven stage and a slower boundary-independent stage as observed in experiments using pigmented and neural epithelial cells from the eyes of seven day chick embryos [64, 65]. The rapid stage leads to a uniform light-cell–medium surface layer and partial bulk cell sorting and the slow stage leads to complete cell sorting. The simulation also reproduces other biological phenomena like chequerboard cell patterns, clumping, engulfment, partial sorting, cell dispersal and vacancy nucleation [59, 60, 61, 64, 65].

## 2.3 Other Applications of the Monte Carlo Approach to tissue-cell populations

Drasdo *et al.* [56, 57, 58] described the stochastic dynamics of tissues of cells with emphasis on epithelial cells and fibroblasts and fibrocytes of the connective tissue. They investigated pattern formation and growth characteristics of such cell populations in culture numerically, using two dimensional Monte Carlo simulations for quasi-two-dimensional aggregates of cells.

Their models employ a simplified coarse grained description of cells, which takes into account the cell shapes only in a statistical sense. Each cell has a centre location and an attached region in space which contains the cell volume and defines the cell shape.

They distinguish two cell classes, inter-phase and mitotic. During the inter-phase, the cell grows steadily until it has doubled its mass, its organelles and DNA content. Then it enters mitosis where it deforms until it completes cell division, whereupon the daughter cells enter the inter-phase. Cells may also migrate and rotate.

The state $\vec{S}_i$ of a cell $i$ is described by its position, its age class, and its shape. The cell position is given by the vector $\vec{r}_i$ of its centre of mass. For an I cell (cell in the inter-phase), the shape is characterised by its radius $R_i$, whereas for an M cell (cell undergoing mitosis), it is the vector $\vec{d}_i$, joining the centres of the corresponding dumbbell which fixes its shape.

Cells interact via a short range potential, $V$. For a pair of cells $i$ and $j$ in the inter-phase

$$V^{II}(i,j;t) = \begin{cases} \infty & \text{for } |\vec{r}_i - \vec{r}_j| \leq R_i(t) + R_j(t) \\ -\epsilon & \text{for } R_i(t) + R_j(t) \leq |\vec{r}_i - \vec{r}_j| \leq R_i(t) + R_j(t) + \delta \\ 0 & \text{otherwise.} \end{cases}$$

During all cell interactions an M-cell is treated like a composite of two, partially

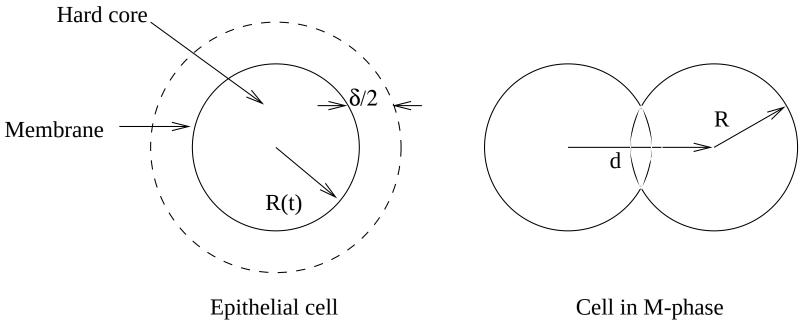


Figure 1: Diagram of a typical cell shape in the I-phase and the typical dumbbell shape of a cell in M-phase.

overlapping spherical cells and the interaction energy between two M-cells is

$$V^{MM}(i,j;t) = \begin{cases} \infty & \text{for} \quad |\vec{r_i}^{(k)} - \vec{r_j}^{(l)}| \le R_i(t) + R_j(t) \\ & \quad \text{with } k,l = 1,2 \\ f(i,k;j,l;t) & \text{for} \quad R_i(t) + R_j(t) \le |\vec{r_i}^{(k)} - \vec{r_j}^{(l)}| \le R_i(t) + R_j(t) + \delta \\ & \quad \text{for at least one } k \in \{1,2\} \text{ and one } l \in \{1,2\} \\ 0 & \text{for} \quad |\vec{r_i}^{(k)} - \vec{r_j}^{(l)}| > R_i(t) + R_j(t) + \delta \\ & \quad \forall i,j \text{ with } i \neq j \text{ and } k,l = 1,2. \end{cases}$$

Here $i, j$ are the cell indices, $k$ $(l)$ is the index for the two overlapping circles forming cell $i$ $(j)$, and $f$ is a function of the interactions between the 4 circles making up the two cells. The interaction between I and M cells is similar.

The total Hamiltonian then is:

$$\mathcal{H} = \sum_{\text{all cell pairs}} V(\vec{S_i}, \vec{S_j}).$$

During a single updating step, only one randomly chosen cell is considered as active and tries to perform one of the following actions $\alpha$:

(i) $\alpha^I \in$ {migration, growth} for I cells, (ii)$\alpha^M \in$ {migration, rotation, deformation} for M cells.

A single migration trial consists of a shift $\vec{r_i} \to \vec{r_i}(1+\delta)$ of cell $i$ in a random direction with a step length which is chosen at random from an interval $[0, \delta r_{max}]$. A rotation trial is defined similarly. During a growth step, the radius of an I cell increases by a random amount $\delta$R$\in[0, \delta R_{max}]$, whereas during a deformation step, the length of $\vec{d}$ increases and at the same time the dumbbell radius decreases to keep the volume of the cell constant.

The trial change is accepted with the same probability as in standard Potts model [66].

This model "performs" wound healing of a skin cut and the spread of a sarcoma (cancer of the connective tissue) across an epithelial boundary, and results are given for these simulations. Drasdo *et al.* then go on to discuss variations of this model, *e.g.* changing the mobility of the I and M cells, and give examples of cells *in vivo* that behave in the manner predicted.

Drasdo and Kree expand on the basic model in other later reports [56, 57].

# 3 Mathematical Model of Avascular Tumour Growth

We now model a three dimensional avascular tumour using an extension of the Potts model used by Glazier *et al.* [59, 60, 61, 64, 65].

## 3.1 The Model

Tumour simulations based on the Extended Potts model include cells which grow and divide, cells which shrink and decay and cells which maintain relatively constant volume. We consider necrotic, quiescent and proliferating tumour cells as distinct cell types, in addition to healthy cells, with different growth rates and volume constraints for each type. Target volumes for healthy and quiescent cells remain constant in time. Target volumes increase for proliferating cells, to simulate growth and decrease for necrotic cells to simulate decay. The volume constraints for proliferating, quiescent and necrotic cells are successively weaker. Accordingly, proliferating cells can grow at the expense of quiescent cells which, in turn, recoup their losses from decaying necrotic cells.

Normal cells have the strongest adhesive bonds with normal cells and tumour-tumour bonds are the weakest, with tumour-normal bonds in between. The resulting surface tension keeps the tumour compact. This hierarchy of binding strengths is consistent with biological evidence, as tumour cells adhere to themselves less strongly than their counterpart normal cells [1, 67]. Although growth and decay rates differ for proliferating, necrotic and quiescent cells, all tumour cells have the same binding properties. Tumour cells express fewer adhesion molecules than normal cells, especially N-CAMs and E-cadherins [67, 68, 69]. In fully transformed cancer cells the expression of cell adhesion molecules is often completely absent [70]. The progressive failure of adhesion during transformation results in rounding of individual cells and loosening of cell-cell bonds in tumours. The intermediate value for normal-tumour cell binding is consistent with the assumption that normal and tumour cells were originally of the same type and hence express the same adhesion molecules, only in different quantity. In this case the heterotypic adhesion is expected to be the geometric mean between the homotypic adhesivities.

Proliferating tumour cells grow in response to the demands of an increasing target volume with mitosis occurring whenever the ratio of surface area to volume for a cell drops below a threshold. This criterion for cell division reflects the fact that cell volume determines the demand for nutrients while cell surface area limits the rate of nutrient absorption. Since tumour cells grow and divide continuously without observing regulatory signals, the simplest assumption is that their growth rate is directly proportional to the supply of nutrients up to some saturating rate. Mombach *et al.* [40, 41] investigated mitosis in plants and showed that this assumption gave good quantitative agreement with experimentally observed cell distributions in plant epithelia. The cell splits in a plane through the centre of mass corresponding to a minimal cross section with all the array elements on one side of the cell assigned a previously unused index. After a split, each daughter cell starts with half the target volume of the parent cell so as not to be unduly stressed by a large deviation from the mandated size of the progenitor. Since, experimentally, mean tumour cell size is comparable to mean normal cell size, we apply mitosis at twice the typical cell size, which corresponds to a area/volume ratio of 0.6.

We do not include the growth of normal cells, since cell division in normal tissue does not affect the tissue volume. Inhibition of cell division in normal tissue keeps the rate of cell division in homeostasis with the rate of cell death. The much slower mitosis of normal cells should not affect the tumour's growth, but can be included in future simulations.

Cells change type in response to a nutrient gradient within the tumour. We assume that the normal tissue is a homogeneous source of nutrient. The concentration of nutrient within the tumour is measured as a function of the distance of the centre of mass of a particular cell from the periphery of the tumour and the total volume of live (and hence nutrient consuming) cells within the tumour. The volume of proliferating cells in the tumour remains roughly constant throughout growth [18] so we require that:

$$\text{volume of proliferating cells} = \frac{4}{3}\pi(R^3 - R_q^3) = A \quad (\text{constant}) \; ,$$

where $R$ is the average tumour radius and $R_q$ is the average outer radius of the quiescent shell. $A$ can be calculated from data on spherical tumours grown *in vitro* [21]. The distance of the first quiescent cell from the edge of the tumour is $R - R_q$, so we choose the critical distance to be $D_q$, where:

$$D_q = R - R_q = \text{ integer part of } \left(\frac{3}{4\pi}\frac{A}{(R^2 + R_q^2)}\right) .$$

The distance of the first dead cell from the periphery $D_d = 4D_q$. This approximation is close to the true, diffusion-determined concentration but is much simpler and computationally faster to implement.

In addition to type changes caused by shifting boundaries between regions within the tumour, individual cells can change type by relocating, as long as they are alive. Since cells are free to move by gradually shifting their boundaries at random, they occasionally migrate to an adjacent region of the tumour. When this migration happens, proliferating and quiescent cells change type according to nutrient availability. Though necrotic cells may undergo passive relocation, they are no longer viable and never revert to quiescence or proliferation.

The growth rate of proliferating cells also depends on nutrient concentration. The growth rate of the cells is:

$$\text{growth rate} = \begin{cases} 0 & \text{if } 0 \leq N \leq N_q; \\ \frac{1}{2}(1 - \frac{N}{N_q})^2 & \text{if } N_q \leq N \leq 3N_q; \\ 2 & \text{otherwise,} \end{cases}$$

where $N_q$ is the critical value of nutrient, below which cells are unable to divide, and is proportional to $R - R_q$, while $N$, the level of nutrient, is proportional to $R - d$, where $d$ is the depth of a cell within the tumour. The depth of a cell is the minimum distance from the centre of mass of the cell to the outer edge of the tumour along each of the three orientations of the array (*i.e.* in the $x$, $y$ and $z$ directions). The increase in volume of the tumour cells is the integer part of the growth rate. This function for growth rate is the simplest continuously differentiable function that has a value of 0 at the outer edge of the quiescent core and 2 at the tumour's edge.

The simulated decay of necrotic cells by reduction of target volume also depends upon depth within the tumour. We assume that cells nearer the centre of the tumour will have been dead longer than those near quiescent cells and therefore will be more likely to have broken down into diffusible compounds and hence will lose volume more readily than those that have just died. So we take the rate of reduction of volume to be proportional to the individual cell's distance from the edge of the necrotic core, up to some saturating rate. Necrotic cells in the outer layer of the core maintain constant volume while cells in the fourth layer from the edge and beyond lose two units of volume at each time step with a linear increase in the decay rate for intervening layers.

Modifications to the Extended Potts model for the purpose of modelling tumours can be summarised by considering changes to the functional dependence of target volumes, cell elasticities and cell types. Cell types and elasticities become a function of nutrient concentration, which varies spatially within the tumour:

$$\begin{array}{ccc} \tau & \longrightarrow & \tau[N] \, , \\ \lambda[\tau] & \longrightarrow & \lambda[\tau, N] \, , \end{array}$$

where $\tau$ is cell type, $\lambda[\tau]$ the membrane elasticity and $N$ is the nutrient concentration. Through dependence on cell type, elasticities have an implicit dependence on nutrient concentration, in addition to an explicit dependence. Also, elasticities have an implicit dependence on position through the spatial variation in nutrient concentration within the aggregate. The target volumes become functions of time:

$$\begin{array}{ccccc} V & \longrightarrow & V[\tau, \sigma, t] \, , & & \\ \frac{dV}{dt} & > & 0 & \text{if} & \text{proliferating,} \\ \frac{dV}{dt} & = & 0 & \text{if} & \text{normal, quiescent,} \\ \frac{dV}{dt} & < & 0 & \text{if} & \text{necrotic,} \end{array}$$

where $V[\tau]$ is the target volume, which depends on cell type as before, but now varies for each cell $\sigma$ since proliferating cells may be at different stages of the mitotic cycle. Despite these modifications, cell configurations are still characterised in terms of stored energy with the usual Monte Carlo dynamics driving rearrangement.

Figure (2) shows a flow diagram of the computer algorithm.

The model of Drasdo *et al.* differ in important respects from the Extended Potts Model. Working in two dimensions, Drasdo and his colleagues describe cells as overlapping circles with short range attraction and hard core repulsion. They employ explicit rules for cell translation and rotation with position and orientation changing in discreet steps. Cell growth and division are handled separately. Binding depends on the proximity of neighbouring cell centres rather than the degree of contact

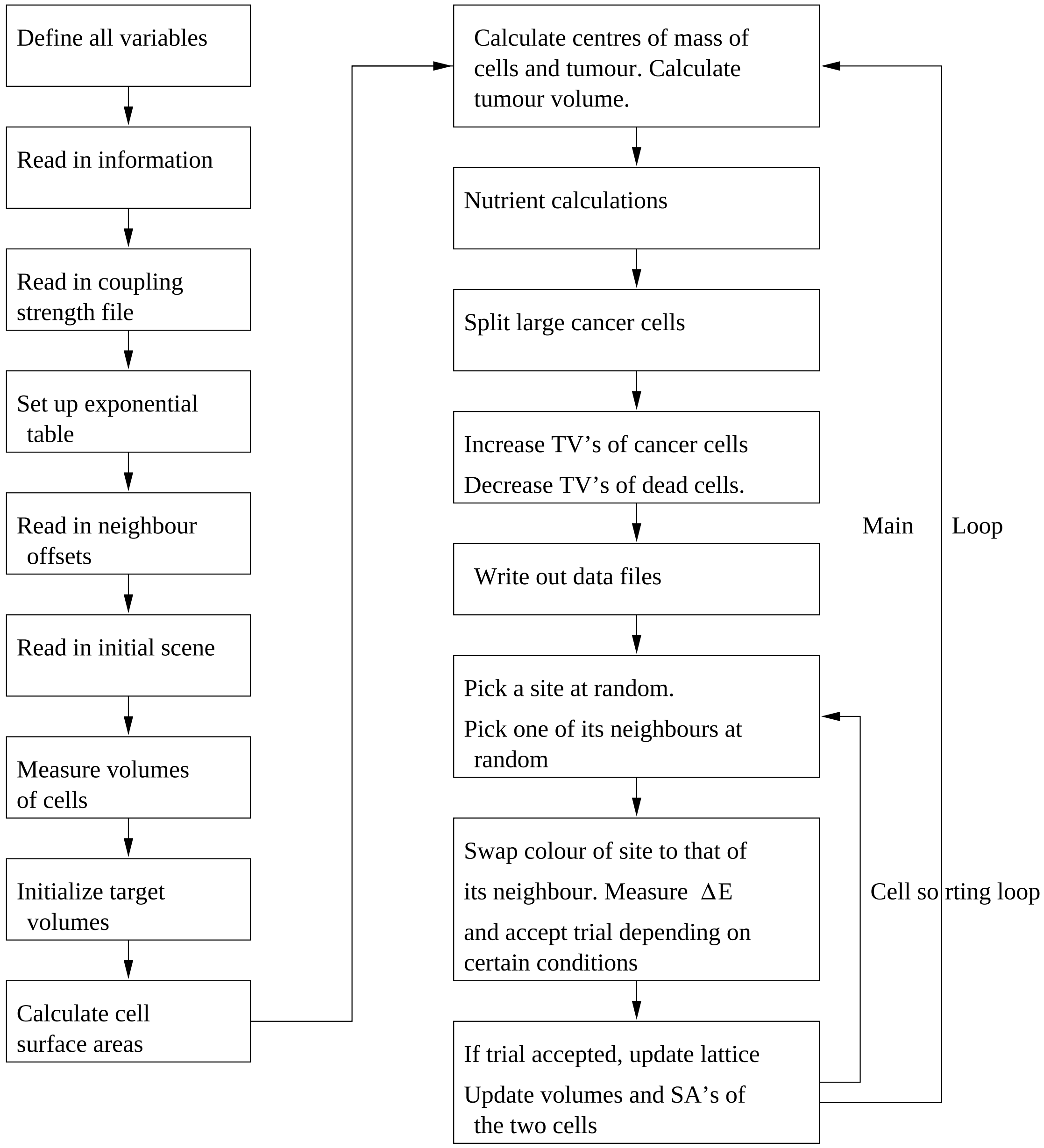


Figure 2: Simple flow diagram of computer algorithm.

between attached membranes. Contrastingly, the lattice of the Extended Potts Model allows cells in three dimensions with almost arbitrary shape. Energy is stored at the boundaries between cells in order to model the binding potential of surface adhesion molecules more directly. Cells translate and rotate in response to gradual boundary adjustment driven by membrane fluctuations without any additional rules. The Extended Potts Model treats cell growth and division as one continuous process governed by nutrient availability.

# 4 Simulation of a Multicell Spheroidal Avascular Solid Tumour

We start off with a small homogeneous aggregate of tumour cells, embedded in normal tissue. All cells are initially set to be cubes, to avoid packing problems, but the dynamics of the model allows them to round quickly to a more natural shape.

The homogeneous source of nutrient models a multi-cell, spheroidal, avascular tumour. To keep the pictures simple, we show a cross section in the X-Y plane, which slices the tumour in two. Figure (3) shows only tumour cells individually and represents all the normal cells by a block of colour. Figure (4) shows only individual normal cells, and represents the tumour as a solid block of colour in the centre of the picture.

Figure (5) shows the tumour at a later time, when the surface tension has rounded both the cells and tumour.

As the tumour grows, the distance of the cells at the centre of the tumour from the periphery becomes large enough that sufficient nutrient can no longer diffuse to them. Inadequately supplied cells become quiescent. Figure (6) and Figure (7) show the tumour with a quiescent core. Again, the picture shows cross sections through the tumour.

Later, the tumour becomes so big that the distance from the edge of the aggregate to the cells at the centre is too large for enough nutrient to diffuse to them and they die. A necrotic core then forms within the quiescent shell. Figure (8) shows the proliferating cells and the position of the cells that have died. Figure (9) shows the normal and quiescent cells, with a solid block of colour in the centre to represent the necrotic core, and a ring of colour for the proliferating cells.

We measure the volume and the average radius of the tumour as it grows. Figure (10) shows the tumour volume versus simulation time (MCS=Monte Carlo Time Steps). Initially, the growth is exponential, then at around 700MCS, when quiescent cells first appear, the growth slows to linear. At 8600MCS, when the necrotic core forms, the growth slows again and eventually ends as the tumour reaches its diffusion limited steady state. This growth is consistent with the experimental evidence. Figure (11) shows the average tumour radius versus simulation time. The width of the shell of quiescent cells is roughly three times the width of the shell of proliferating cells, which is in good agreement with histological data [18]. We can change this relative thickness by varying the ratio $D_q/D_d$. The top picture in Figure (12) shows the growth of the outer radius of the tumour and the bottom shows the

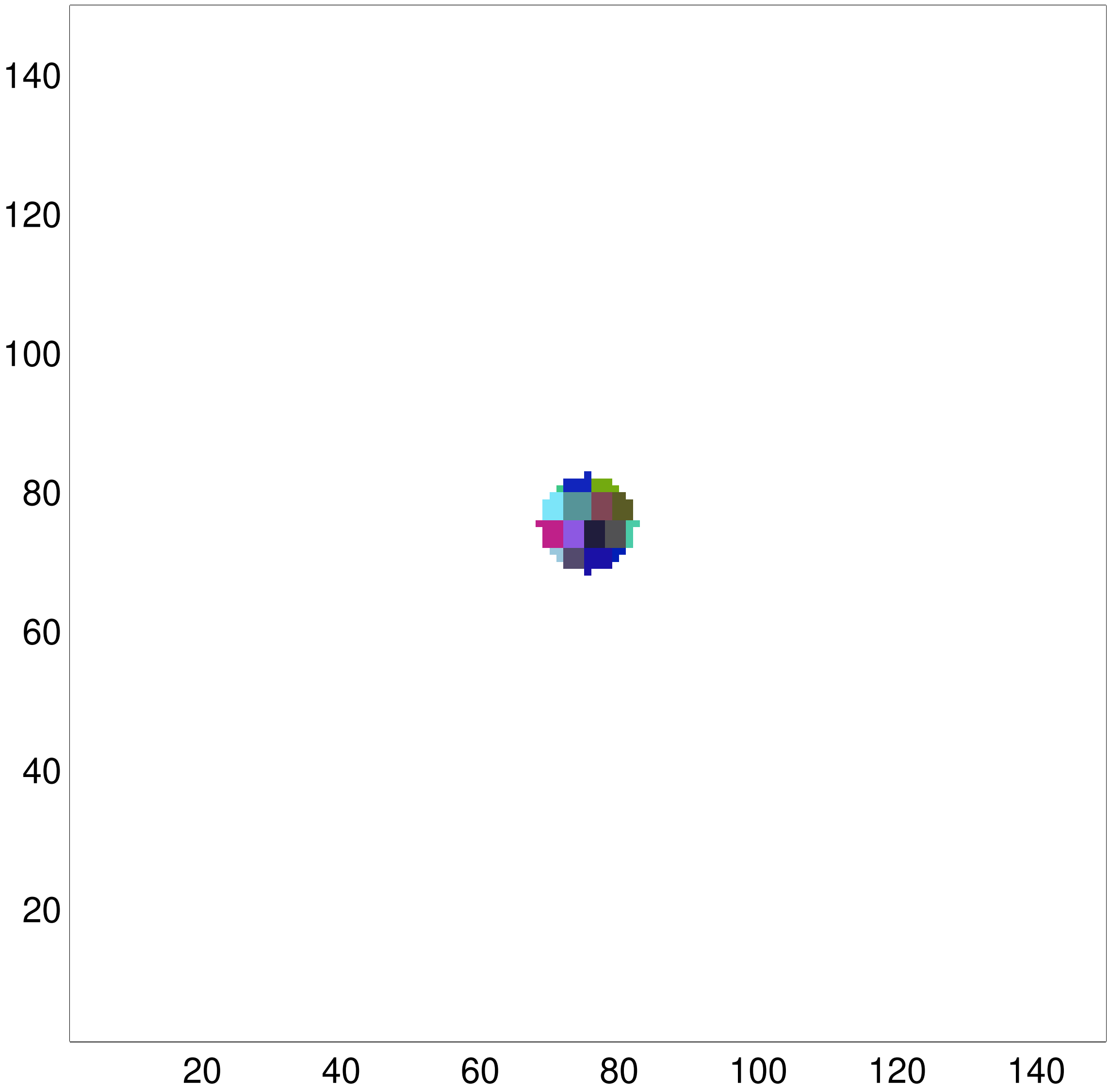


Figure 3: Cross section of the initial configuration, showing cancer cells only.

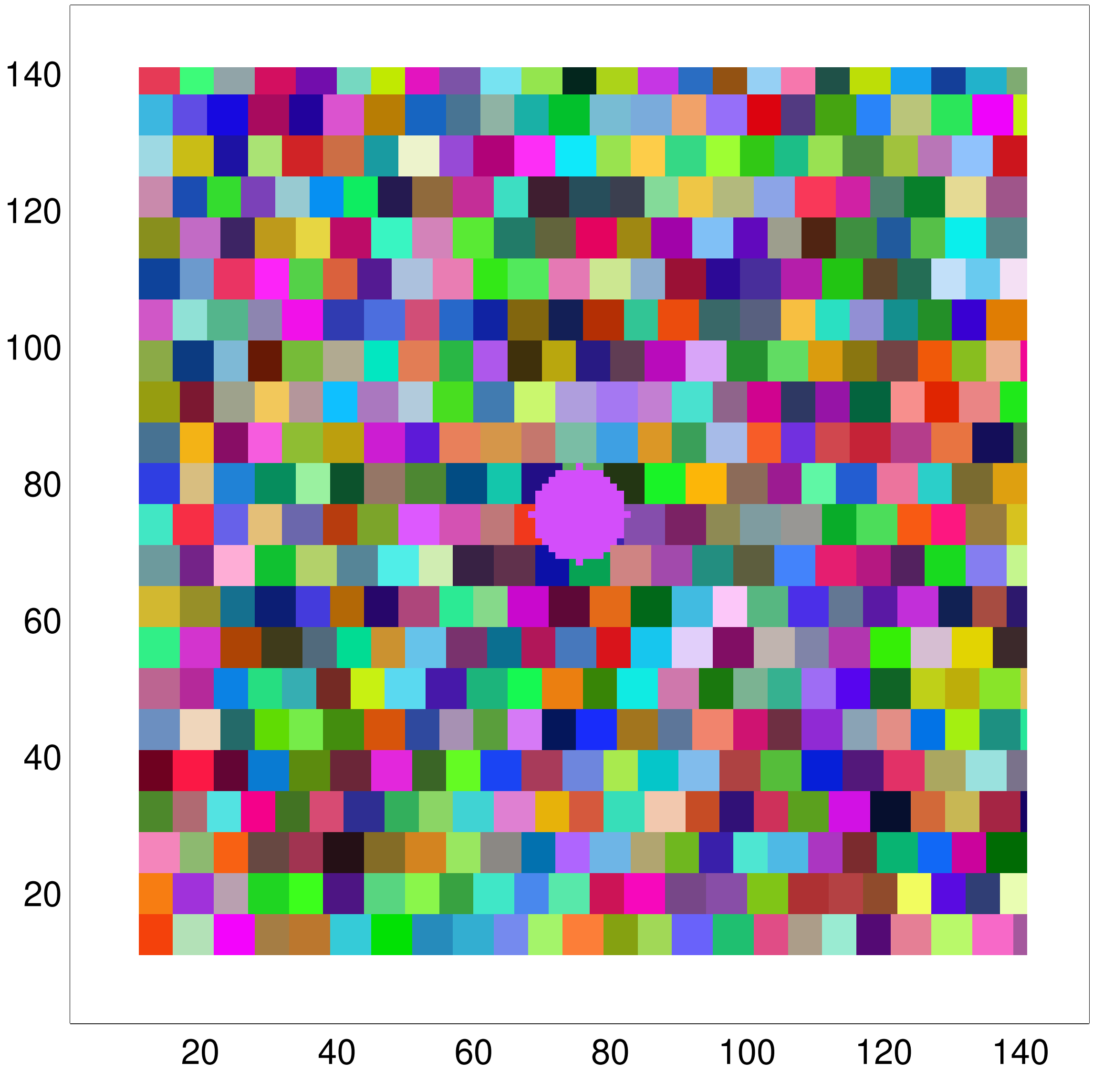


Figure 4: Cross section of the initial configuration, showing normal cells only.

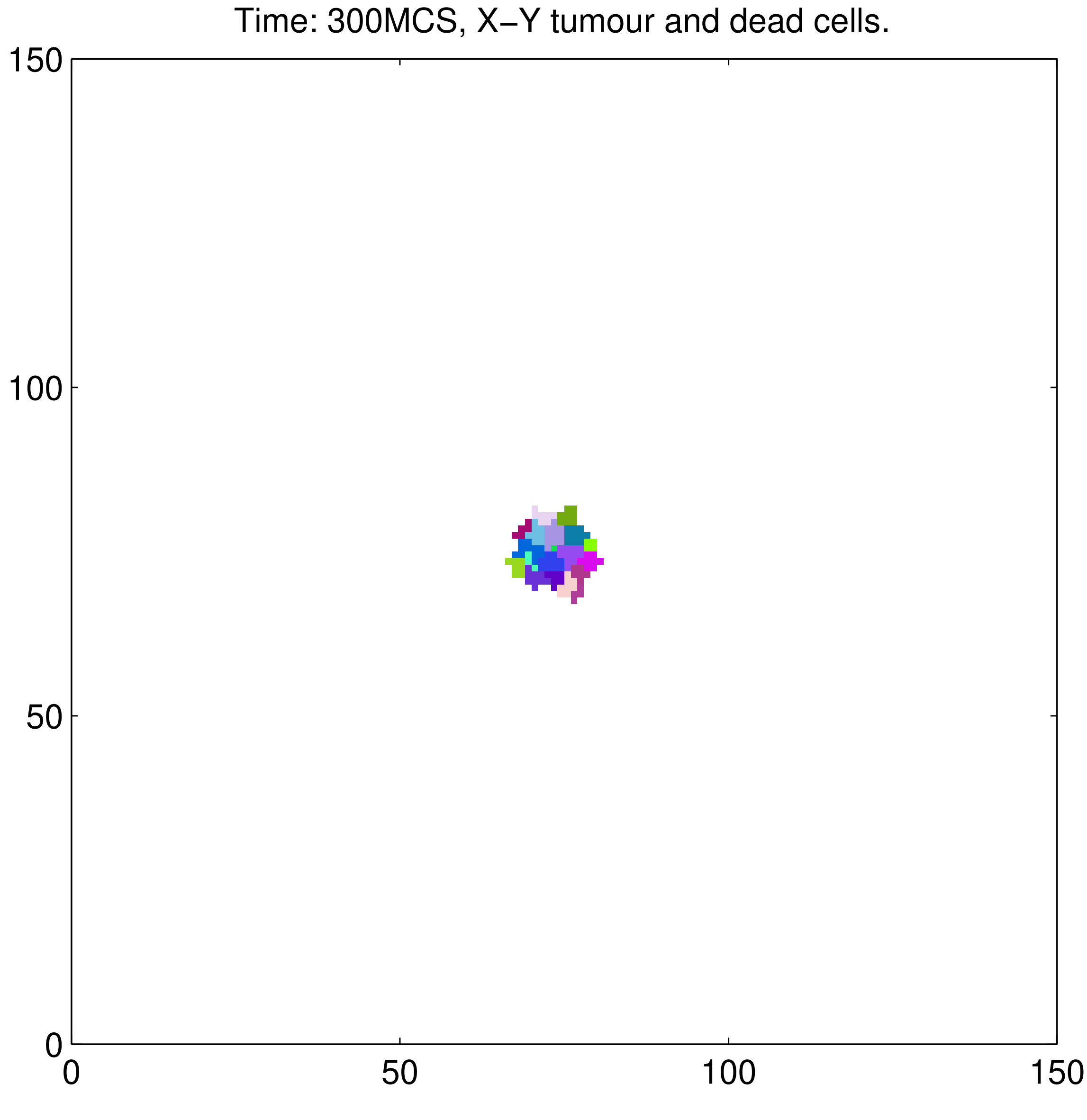


Figure 5: Cross section of rounded configuration, showing proliferating tumour cells only.

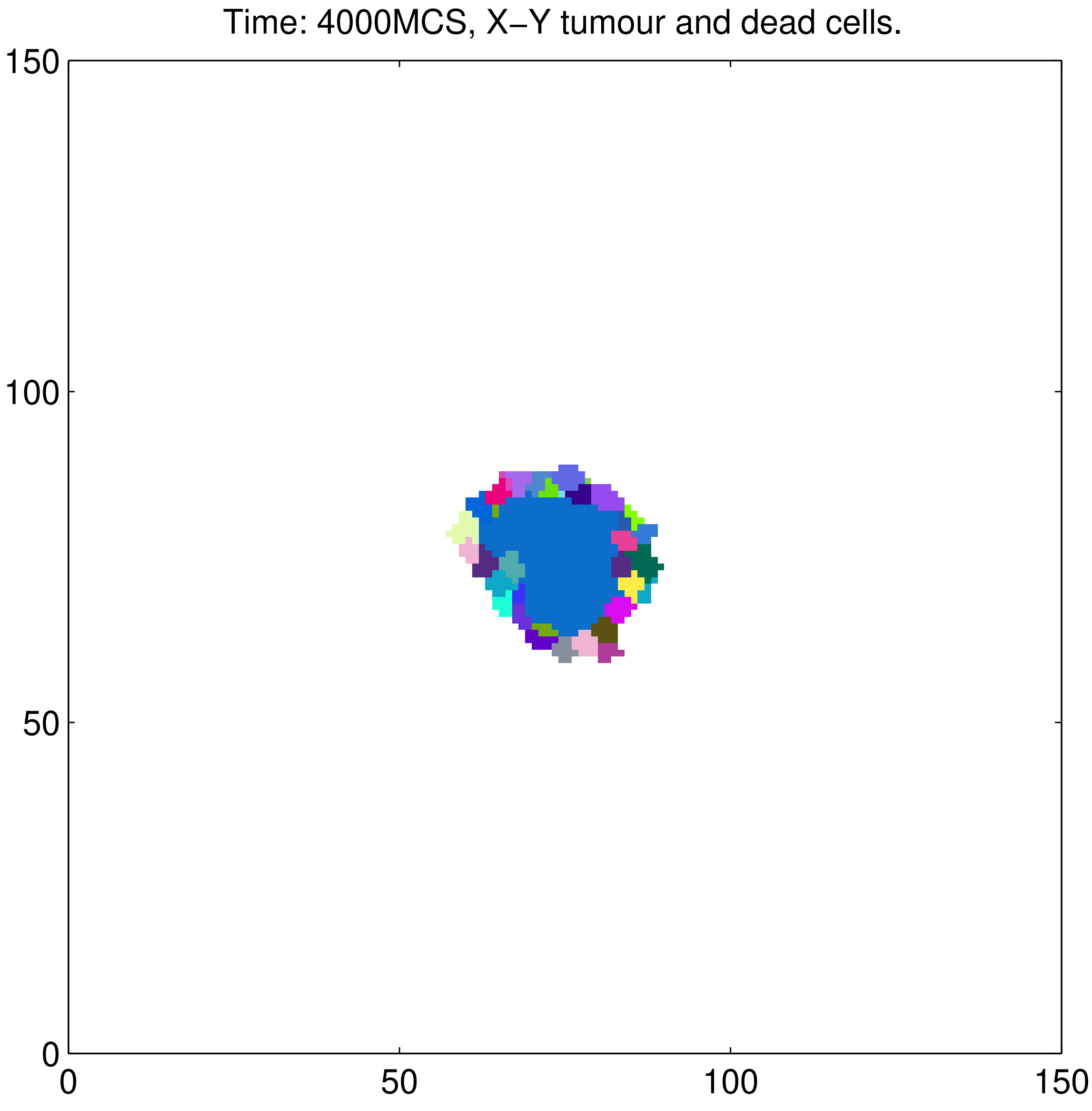


Figure 6: Cross section of tumour, showing proliferating tumour cells only.

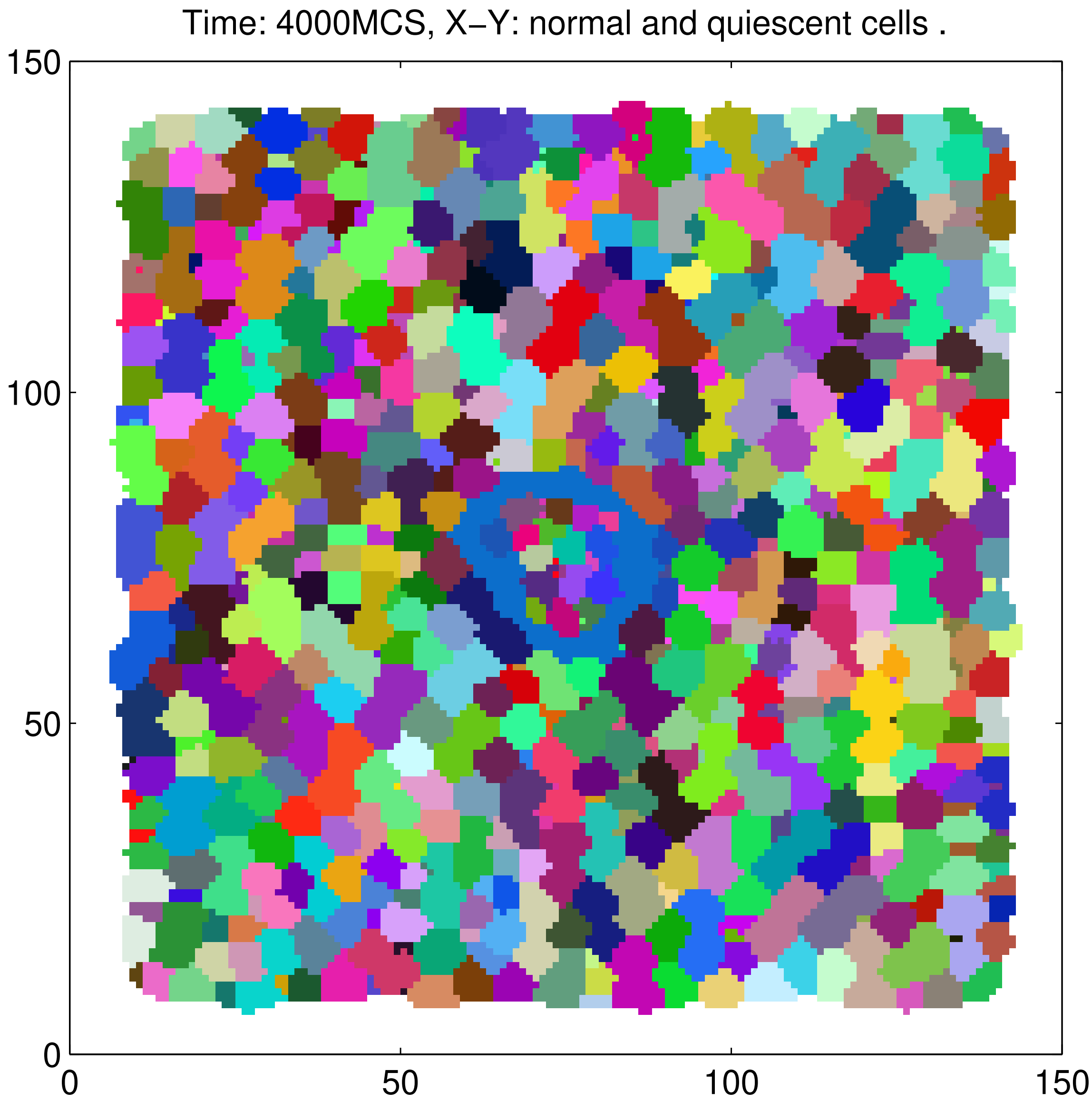


Figure 7: Cross section of tumour, showing normal cells and quiescent tumour cells only.

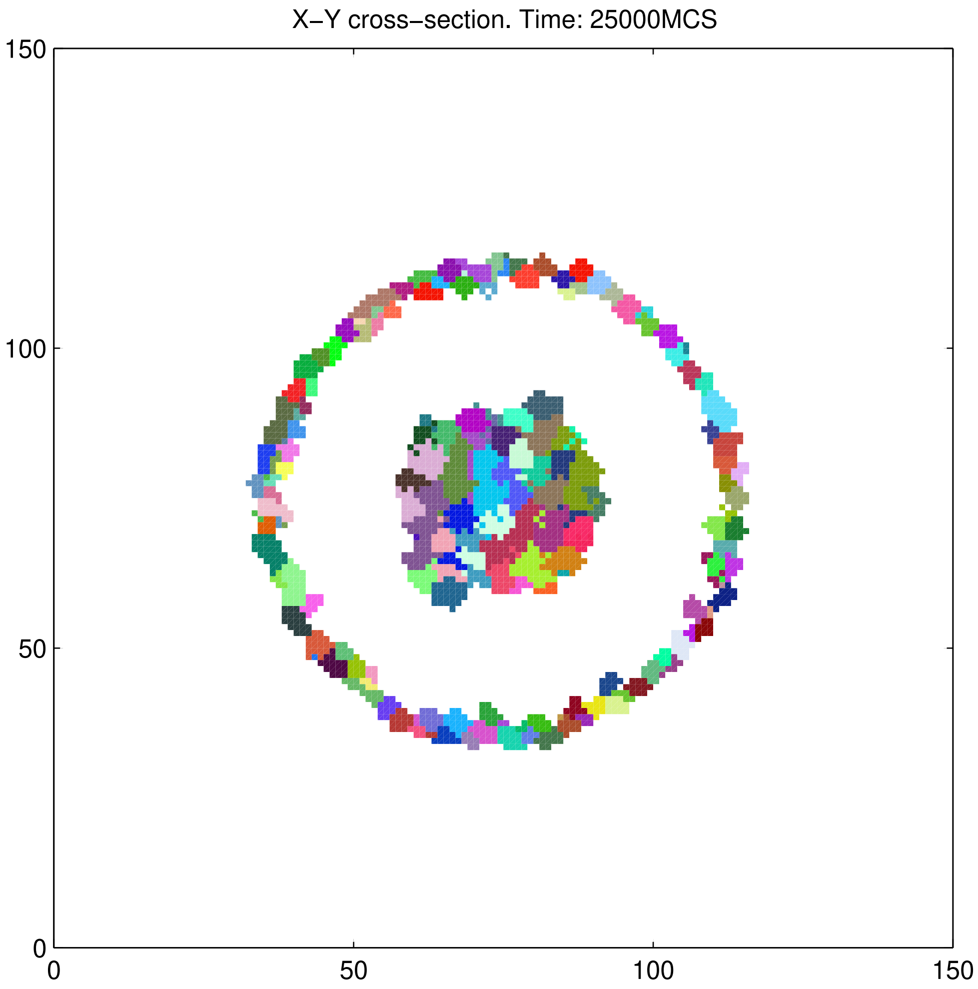


Figure 8: Cross section of tumour, showing proliferating tumour and necrotic cells only.

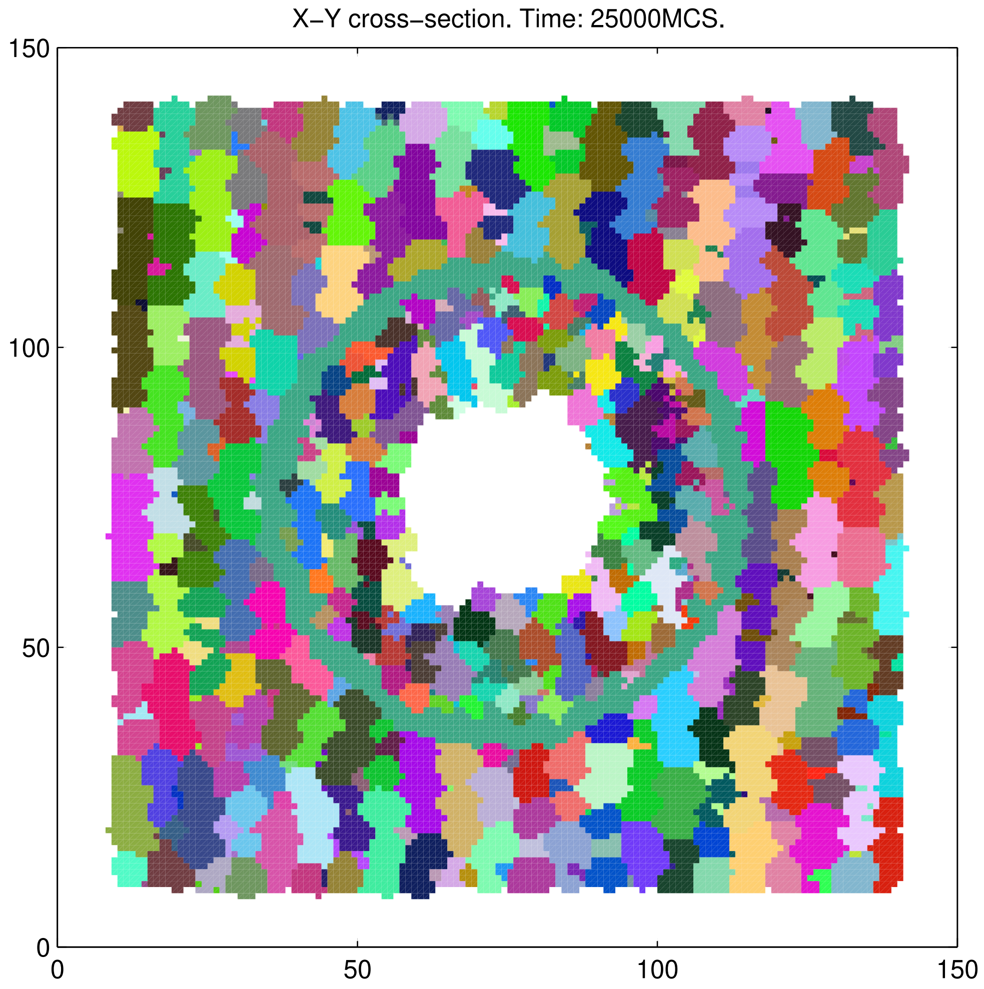


Figure 9: Cross section of tumour, showing normal and quiescent cells only.

graph obtained by Folkman and Hochberg in their experiments on the growth of multicellular spheroids [21].

# 5 Discussion

The Potts Model has proven useful in simulating cell movement. It includes features often neglected in the simplest models of tumour growth, such as cell-cell adhesion. However, we have made many simplifications. Our model of the adhesive properties of cells was as simple as possible. We concentrated on the essential features of the growth of a solid avascular tumour *in vivo*. We assumed that normal tissue surrounding a tumour is homogeneous, that the periphery supplies nutrient uniformly, that the concentration of nutrient in the tumour depends only on the distance from the tumour surface and that a single nutrient largely controls tumour growth. We neglected orientation dependent mechanical and adhesive properties of cells.

Despite these assumptions, our model simulates avascular tumour growth well, reproducing experimental results for the increase of tumour volume.

Also, all of our tumour cells are equally aggressive in their growth and all have the same adhesivity. In a real tumour, some cells will be further down the malignant development pathway than others, so they will vary in their growth rate and adhesivity throughout the tumour. When a tumour cell divides, its daughters do not always have the same properties as the parent [67, 1]. For example, daughter cells may be more aggressive in their growth and also adhere less to other tumour cells, thus being more likely to break away from the tumour mass into the normal tissue. Our model could be developed to include metastasis by allowing the daughter cells to have randomly fluctuating growth rates and adhesivities with respect to the values of their parent cell, according to a probability matrix. In this case we could simulate the evolution of a true metastatic, though avascular cancer.

Normal tissue is also not homogeneous - it contains extracellular matrix, fibrin, collagen, blood vessels *etc...*, so normal tissue is not a homogeneous source of nutrient. We are currently developing the model to include nutrient diffusing to the tumour from nearby blood vessels, through heterogeneous tissue.

When a tumour reaches its diffusive equilibrium, it can no longer increase in size, unless it gets its own blood supply. It does this by releasing a chemical called Tumour Angiogenesis Factor into the surrounding tissue, which causes nearby blood vessels to form sprouts, which grow into new capillaries. These eventually penetrate the tumour mass and subsequent growth is exponential [8, 11, 21, 24, 71, 72]. We plan to extend our model to include these features.

**Acknowledgements**

E.L.S. acknowledges the support of an EPSRC studentship for this research.
J.A.G. and M.Z. acknowledge support for this research from the National Science Foundation under grants, INT91-01345, DMR92-57011, CTS96-01691, INT96-03035 and INT98-02417, and from the ACS/PRF and Royal Irish Academy.

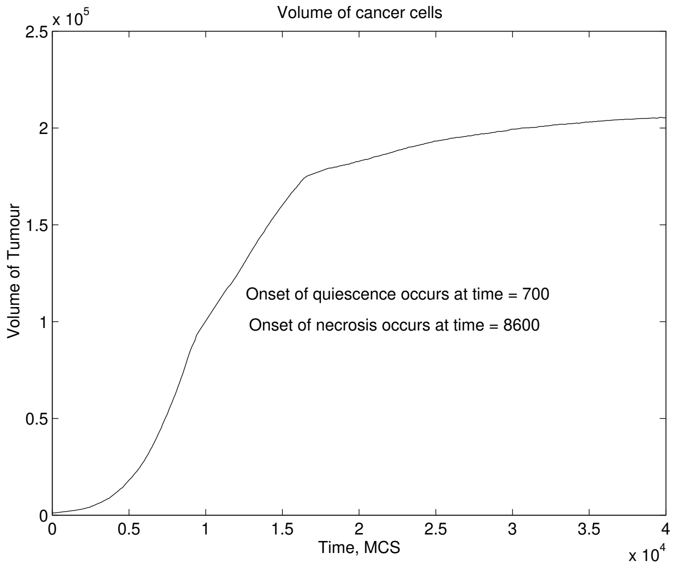


Figure 10: Volume of the growing tumour

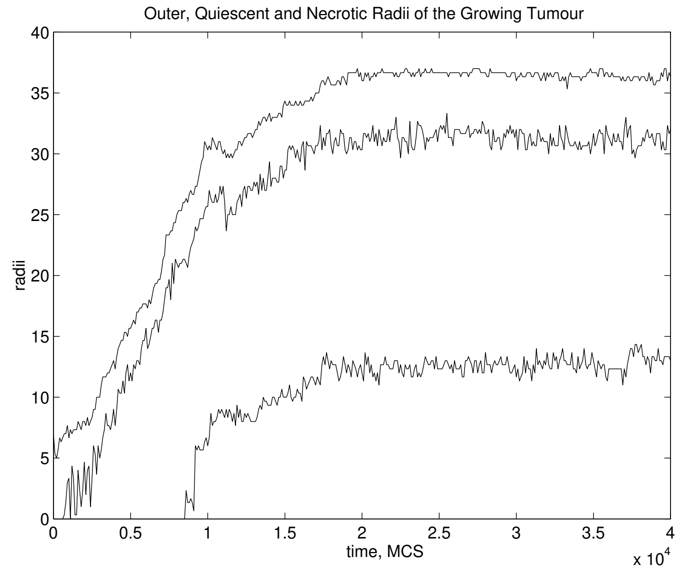


Figure 11: Radii of the growing tumour

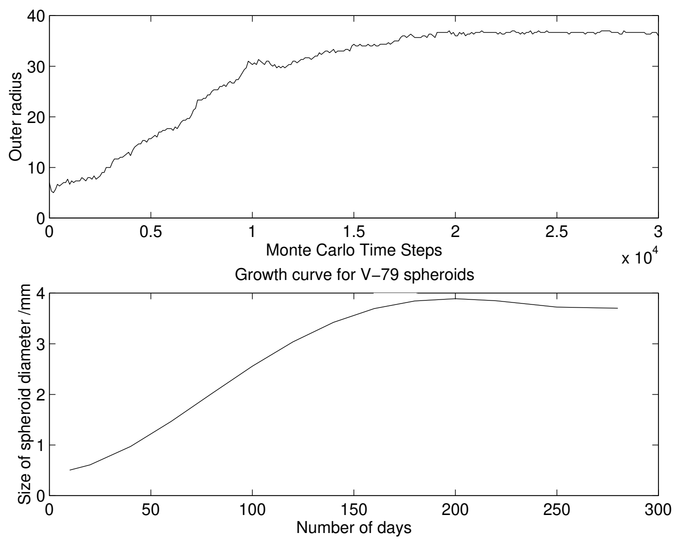


Figure 12: Comparison of the growth of tumour Radius with Folkman and Hochberg's measurements

# References


[1] A.D. Wyllie. Growth and neoplasia. In R.N.M.Macsween and K.Whaley, editors, *Muir's Textbook of Pathology*, chapter 10. Edward Anderson, (1992).

[2] L. Wolpert. *The Triumph of the Embryo*, chapter 11 - Cell multiplication and cancer. Oxford University Press, (1993).

[3] C. Van Waes, D.M. Surh, Z. Chen, M. Kirby, J.S. Rhim, R. Brager, R.B. Sessions, J. Poore, G.T. Wolf, and T.E. Carey. Increase in suprabasilar integrin adhesion molecule expression in human epidermal neoplasms accompanies increased proliferation occurring with immortalization and tumor progression . *Cancer Research*, **55**:5434–5444, (1995).

[4] S.A. Maxwell, D. Capp, and S.A. Acosta. Telomerase activity in immortalized endothelial cells undergoing p53-mediated apoptosis. *Biochemical and Biophysical Research Communications*, **241**:642–645, (1997).

[5] J.W. Shay. Telomerase in human development and cancer. *Journal of Cellular Physiology*, **173**:266–270, (1997).

[6] S.H. Kauffman, editor. *Apoptosis: Pharmacological Implications and Therapeutic Opportunities, Advances in Pharmacology, volume 41.* Academic Press, London, (1997).

[7] R. Langer. Isolation of a cartilage factor that inhibits tumor neovascularisation and growth. *Science*, **193**:70–72, (1976).

[8] J. Folkman. Tumor angiogenesis: therapeutic implications. *New England Journal of Medicine*, **285**:1182–1186, (1971).

[9] W.R. Inch, J.A. McCredie, and R.M. Sutherland. Growth of nodular carcinomas in rodents compared with multicell spheroids in tissue culture. *Growth*, **34**:271–282, (1970).

[10] R.M. Sutherland, W.R. Inch, and J.A. McCredie. Growth of multicell spheroids in tissue culture as a model of nodular carcinomas. *Journal of the National Cancer Institute*, **46**:113–120, (1971).

[11] J. Folkman, E. Merler, C. Abernathy, and *et al.* Isolation of a tumour factor responsible for angiogenesis. *Journal of Experimental Medicine*, **133**:275–288, (1971).

[12] R.H. Thomlinson and L.H. Gray. The histological structure of some human lung cancers and the possible implications for radio therapy. *British Journal of Cancer*, **9**:539–549, (1955).

[13] J.P. Freyer and R.M. Sutherland. Regulation of growth saturation and development of necrosis in EMT6/Ro multicellular spheroids by the glucose and oxygen supply. *Cancer Research*, **46**:3513–3520, (1986).

[14] J.P. Freyer and P.L. Schor. Regrowth of cells from multicell tumour spheroids. *Cell Tissue Kinetics*, **20**:249, (1987).

[15] K. Groebe and W. Mueller-Klieser. Distributions of oxygen, nutrient and metabolic waste concentrations in multicellular spheroids and their dependence on spheroid parameters. *European Biophysics Journal*, **19**:169–181, (1991).

[16] A.D. Conger and M.C. Ziskin. Growth of mammalian multicellular tumour spheroids. *Cancer Research*, **43**:556–60, (1983).

[17] J.P. Freyer, E. Tustanoff, A.J. Franko, and R.M. Sutherland. In situ oxygen consumption rates of cells in V-79 multicellular spheroids during growth. *Journal of Cellular Physiology*, **118**:53–61, (1984).

[18] D.L.S McElwain and G.J. Pettet. Cell migration in multicell spheroids: swimming against the tide. *Bulletin of Mathematical Biology*, **55**:655–674, (1993).

[19] P.W. Vaupel, S. Frinak, and H.I. Bicher. Heterogeneous oxygen partial pressure and pH distribution in c3H mouse mammary adenocarcinoma. *Cancer Research*, **41**:2008–13, (1981).

[20] J.P. Freyer. Role of necrosis in regulating the growth saturation of multicell spheroids. *Cancer Research*, **48**:2432–9, (1988).

[21] J. Folkman and M. Hochberg. Self-regulation of growth in three dimensions. *Journal of Experimental Medicine*, **138**:745–753, (1973).

[22] J.F.R. Kerr. Shrinkage necrosis; a distinct mode of cellular death. *Journal of Pathology*, **105**:13–20, (1971).

[23] J.F.R. Kerr, Wyllie, and A.R. Currie. Apoptosis: A basic biological phenomenon with wide-ranging implications in tissue kinetics. *British Journal of Cancer*, **26**:239–257, (1972).

[24] N. Paweletz and M. Knierim. Tumor-related angiogenesis. *Critical reviews in Oncology/Hematology*, **9**:197–242, (1989).

[25] M.S. Steinberg. On the mechanism of tissue reconstruction by dissociated cells, I. Population kinetics, differential adhesiveness, and the absence of directed migrations. *Proceedings of the National Academy of Sciences U.S.A.*, **48**:1577, (1962).

[26] M.S. Steinberg. On the mechanism of tissue reconstruction by dissociated cells, III. Free energy relations and the reorganization of fused, heteronomic tissue fragments. *Proceedings of the National Acadamy of Sciences U.S.A.*, **48**:1769, (1962).

[27] M.S. Steinberg. Mechanism of tissue reconstruction by dissociated cells, II: Time course of events. *Science*, **137**:762–3, (1962).

[28] P. Armstrong. Cell sorting out: The self-assembly of tissues in vitro. *Critical Reviews in Biochemistry and molecular Biology*, **24**:119–149, (1989).

[29] M. Dan-Sohkawa, H. Yamanaka, and K. Watanabe. Reconstruction of Bipinnaria larvae from dissociated embryonic cells of the starfish, Asterina-Pectinifera. *Journal of Embryology and Experimental Morphology*, **94**:47–60, (1986).

[30] A. Gierer, S. Berking, H. Bode, C.N. David, K. Flok, G. Hansmann, H. Schaller, and E. Trenkner. Regeneration of hydra from reaggregated cells. *Nature*, **239**:98–101, (1972).

[31] K. Noda. . *Zool. Mag.*, **80**:99, (1971).

[32] P. Townes and J. Holtfreter. . *Journal of Experimental Zoology*, **128**:53, (1955).

[33] J. Holtfreter. . *Review of Cancer Biology*, **3**:220, (1944).

[34] H.V. Wilson. . *Journal of Experimental Zoology*, **5**:245, (1907).

[35] J. Holtfreter. . *Arch. Exptl. Zellforsch. Gewebezuecht*, **23**:169, (1900).

[36] M.S. Steinberg. Does differential adhesion govern self-assembly processes in histogenesis? Equilibrium configurations and the emergence of a hierarchy among populations of embryonic cells. *Journal of Experimental Zoology*, **173**:395, (1970).

[37] U. Technau and T.W. Holstein. Cell sorting during the regeneration of hydra from reaggregated cells. *Developmental Biology*, **151**:117–127, (1992).

[38] M.P. Sarras, Z. Xiaoming, J.K. Huff, M.A. Accaviti, P.L. St John, and D.R. Abrahamson. Extracellular-matrix (mesoglea) of hydra-vulgaris .3. formation and functions during morphogenesis of hydra cell aggregates. *Developmental Biology*, **157**:383–398, (1993).

[39] S.E. Fraser, C.R. Green, H.R. Bode, and N.B. Gilula. Selective disruption of gap junctional communication interferes with a patterning precess in hydra. *Science*, **237**:49–55, (1987).

[40] J.C.M. Mombach, R.M.C. Dealmeida, and J.R. Iglesias. Mitosis and growth in biological tissues. *Physics Review E*, **48**:598–602, (1993).

[41] J.C.M. Mombach, R.M.C. Dealmeida, and J.R. Iglesias. 2-cell correlations in biological tissues. *Physics Review*, **47**:3712–3716, (1993).

[42] F. Graner. Can surface adhesion drive cell rearrangement? Part I: biological cell-sorting. *Journal of Theoretical Biology*, **164**:455–476, (1993).

[43] R.A. Foty, G. Forgacs, C.M. Pfleger, and M.S. Steinberg. Liquid properties of embryonic tissues - measurement of interfacial tensions. *Physical Review Letters*, **72**:2298–2301, (1994).

[44] A. Moscona. Development of heterotypic combinations of dissociated embryonic chick cells. *Proceedings of the Society for Experimental Biology and Medicine*, **92**:410–416, (1956).

[45] D. McClay and C. Ettensohn. Cell adhesion in morphogenesis. *Annual Review of Cell Biology*, **3**:319–345, (1987).

[46] M. Robertson, J. Armstrong, and P. Armstrong. Adhesive and non-adhesive membrane domains of amphibian embryo cells. *Journal of Cell Science*, **44**:19–31, (1980).

[47] K. Nubler-Yung and B. Mardini. Insect epidermis - polarity patterns after grafting result from divergent cell adhesions between host and graft tissue. *Development*, **110**:1071–1079, (1990).

[48] S. Newman and W. Comper. Generic physical-mechanisms of morphogenesis and pattern formation. *Development*, **110**:1–18, (1990).

[49] M. Takeichi. Cadherin cell-adhesion receptors as a morphogenetic regulator. *Science*, **251**:1451–1455, (1991).

[50] S.E. Koonin and D.C. Meredith. *Computational Physics: FORTRAN version*, chapter 8 - Monte Carlo Methods, pages 197–220. Addison-Wesley, (1990).

[51] F. Haessner. *Recrystalization of metallic materials*, page 3. Riederer Verlag, Stuttgart, (1978).

[52] M.P. Anderson, D.J. Srolovitz, G.S. Grest, and P.S. Sahni. Computer simulation of grain growth - I. kinetics. *Acta Metallica*, **32**:783–791, (1984).

[53] J.A. Glazier, M.P. Anderson, and G.S. Grest. Coarsening in the 2-dimensional soap froth and the large Q-Potts-model - a detailed comparison. *Philosophical Magazine B-Physics of Condensed Matter Structural Electronic Optical and Magnetic Properties*, **62**:615–645, (1990).

[54] D. Weaire, B. Bolton, P. Molho, and J.A. Glazier. Investigation of an elementary model for magnetic froth. *Journal of Physics: Condensed Matter*, **3**:2101–2114, (1991).

[55] N.J. Savill and P. Hogeweg. Modelling morphogenesis: From single cells to crawling slugs. *Journal of Theoretical Biology*, **184**:229–235, (1997).

[56] D. Drasdo. Growing tissue cell populations: a stochastic model based on the Monte Carlo method. Technical report, Max-Planck-Institut für Kolloid- und Grenzflächenforschung, Kantstr. 55, D-14513 Teltow, Berlin, Germany. e-mail = Drasdo@mpikg-teltow.mpg.de, (1995).

[57] D. Drasdo and R. Kree. Simulated tissue: a condensed matter approach to growing cell assemblies and histological processes. Technical report, Max-Planck-Institut, Teltow and Inst.f. Theoretic. Physik, Georg-August Universität, address same as above, (1995).

[58] D. Drasdo, R. Kree, and J.S. McCaskill. Monte Carlo approach to tissue-cell populations. *Physical review E*, **52**:6635–6657, (1995).

[59] F.G. Graner and J.A. Glazier. Simulation of biological cell sorting using a two-dimensional extended Potts model. *Physical Review Letters*, **69**:2013–2016, (1992).

[60] J.A. Glazier and F. Graner. Simulation of the differential adhesion driven rearrangement of biological cells. *Physical Review E*, **47**:2128–2154, (1993).

[61] J.A. Glazier. The thermodynamics of cell sorting. *Bussei Kenkyu*, **65**:691–700, (1995).

[62] J.C.M. Mombach, J.A. Glazier, R.C. Raphael, and M. Zajac. Quantitative comparison between differential adhesion models and cell sorting in the presence and absence of fluctuations. *Physical Review Letters*, **75**:2244–2247, (1995).

[63] J.C.M. Mombach and J.A. Glazier. Single cell motion in aggregates of embryonic cells. *Physical Review Letters*, **76**:3032–3035, (1996).

[64] J.C.M. Mombach and J.A. Glazier. Single cell motion in random aggregates of embryonic cells. *Physical Review Letters*, **76**:3032–3035, (1995).

[65] J.A. Glazier, R.C. Raphael, F Graner, and Y Sawada. The Energetics of Cell Sorting in Three Dimensions. In D. Beysens, M.A. Felix, G. Forgacs, and F. Gaill, editors, *Interplay of Genetic and Physical Processes in the Development of Biological Form*, pages 54–61. Springer, (1995).

[66] N. Metropolis, A.W. Rosenbluth, M.N. Rosenbluth, A.H. Teller, and E. Teller. Equation of state calculations by fast computing machines. *Journal of Chemical Physics*, **21**:1087, (1953).

[67] G.L. Nicholson. Cancer metastasis: tumor cell and host organ properties important in metastasis to specific secondary sites. *Biochimica et Biophysica Acta*, **948**:175–224, (1988).

[68] Masayuki Miyasaka. Cancer metastasis and adhesion molecules. *Clinical orthopaedics and related research*, **312**:10–18, (1995).

[69] W.G. Stetler-Stevenson, S. Aznavoorian, and L.A. Liotta. Tumor cell interactions with the extracellular matrix during invasion and metastasis. *Annual Review of Cell Biology*, **9**:541–573, (1993).

[70] D.I. Kleinerman, P. Tronsco, S-H Lin, L.L Pisters, E.R. Sherwood, T. Brooks, A.C. von Eschenbach, and J-T Hsieh. Consistent expression of an epithelial cell adhesion molecule (C-CAM) during human prostate cancer development and loss of expression in prostrate cancer: implication as a tumour suppressor. *Cancer Research*, **55**:1215–1220, (1995).

[71] D.H. Ausprunk and J. Folkman. Migration and proliferation of endothelial cells in preformed and newly formed blood vessels during tumor angiogenesis. *Microvascular Research*, **14**:53–65, (1977).

[72] J. Folkman. Angiogenesis in cancer, vascular, rheumatoid and other diseases. *Nature Medicine*, **1**:21–31, (1995).